Analysis of positive muon data from μCap Run 8

Frederick Gray, Pomona College / University of California, Berkeley

October 2, 2006

Two small corrections after the version initially posted:

- Missing t added to equation 2.
- Clarification that a blinding offset has been applied.

1 Run subsets

Positive muon data were taken in a number of the subsets of the run that were defined by Francoise Mulhauser:

Designation	Statistics	First-last runs	TPC voltage	Comments
Prod-50	2.9×10^8	11918-14186	5.0 kV	
Prod-48	1.6×10^8	14188-14446	4.8 kV	
CalibD2-48	7.6×10^7	14949-15033	4.8 kV	Deuterium-doped gas
Prod-51	3.5×10^7	10858-11156	5.1 kV	Apparent problem with μSR magnet
Prod-52	6.3×10^6	11382-11390	5.2 kV	Negligibly small

This report examines separately two subsets of comparable statistics: Prod-50, and the sum of Prod-48 and CalibD2-48, which will be called All-48.

2 Muon spin rotation parameters

The positive muon beam that is stopped in the TPC is highly polarized. The spins of the stopped muons are rotated as a function of time by the applied magnetic field. Parity violation in the weak interaction causes the decay positrons to preferentially follow the direction of the muon spin. The result is that the simple exponential decay curve (plus flat background)

$$f(t) = Ne^{-\lambda t} + B \tag{1}$$

is modified to

$$f(t) = Ne^{-\lambda t}\left[1 - P(t)(A_c \cos(\omega_{\mu SR} t) + A_s \sin(\omega_{\mu SR} t)\right] + B \tag{2}$$

The functional form of the polarization $P(t)$ depends on the distribution of magnetic fields experienced by the muon population. Exponential and Gaussian forms may prove to be good approximations:

$$P_{exp}(t) = e^{-t/\tau_{\mu SR}} \tag{3}$$

or

$$P_{gaus}(t) = e^{-t^2/2T_{\mu SR}} \tag{4}$$

The procedure that is used to determine the μSR frequency from the data is the following:

- For each of the eight opposing pairs of eSC counters (1 and 9, 2 and 10, etc.), subtract one from the other, yielding spectra like the ones in Figure 1.

- Fit each spectrum to the usual functional form of Equation 2, with the decay rate held fixed at $\lambda = 454.734$ kHz. This value (to which a blinding offset has been added for this report) is the result of a naive fit of the Prod-50 time spectrum (summed over gondolas) to the functional form of Equation 1. A typical set of fit parameters is shown in Figure 2.

- Construct an appropriately weighted average of the eight fitted frequencies – in practice, by fitting a constant to these values.

With only the usual fiducial volume cut in the TPC, the fitted μSR frequency is not stable. Figure 4 shows the fitted frequency as a function of fit start time for this case. My hypothesis was that the start-time dependence was due to the interference of a wide range of μSR frequencies with differing envelopes from the nonuniform applied magnetic field in the TPC. In order to determine the uniformity of this field, I had previously divided it into $3\times3\times3$ cm cubes and independently fit the μSR frequency for muon stops in each cube. The result, illustrated in Figure 3, demonstrates that the variation of the magnetic field in z is significantly larger than in x or y. Indeed, only the corners of the TPC show large differences in the field relative to the center.

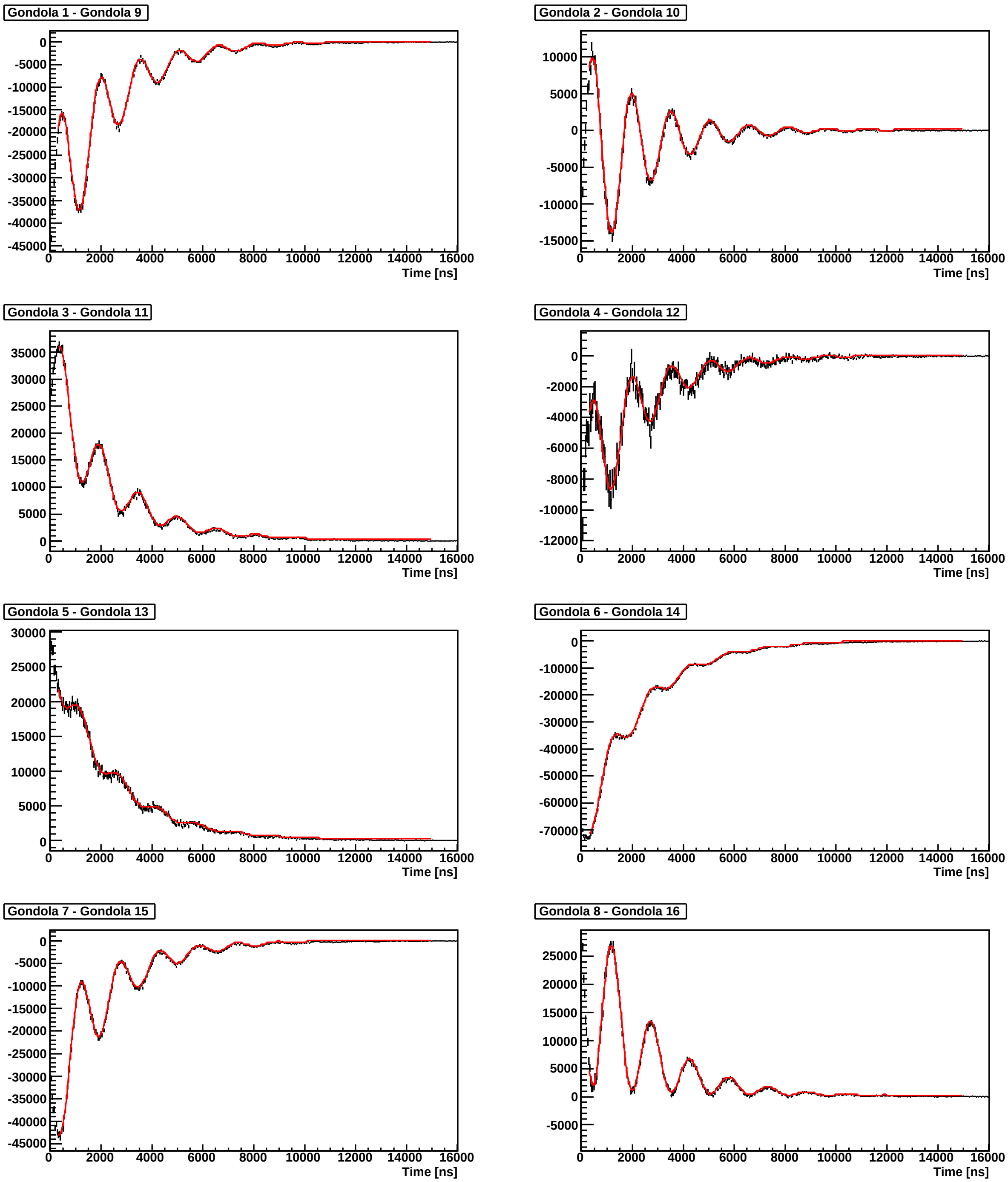

Figure 1: Differences of opposing gondola pairs, constructed to emphasize the μSR modulation, with fits superimposed on the raw count differences. (Prod-50 data, $r < 60$ mm, 60 mm $< z <$ 210 mm).

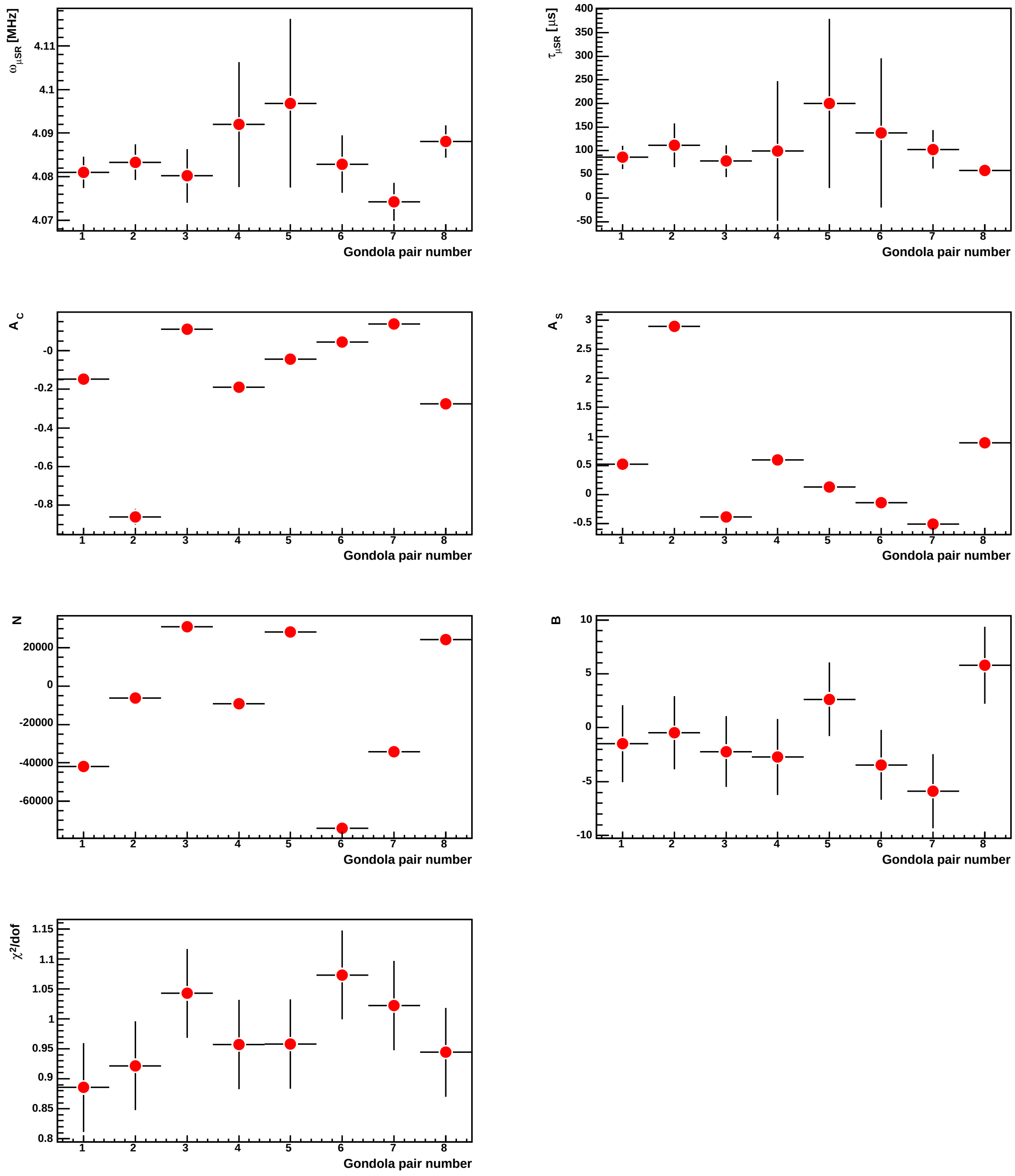

Figure 2: Typical μSR fit parameters for each gondola pair. (Prod-50 data, $r < 60$ mm, 60 mm $< z <$ 210 mm, 320 ns $< t <$ 15 μs, exponential form).

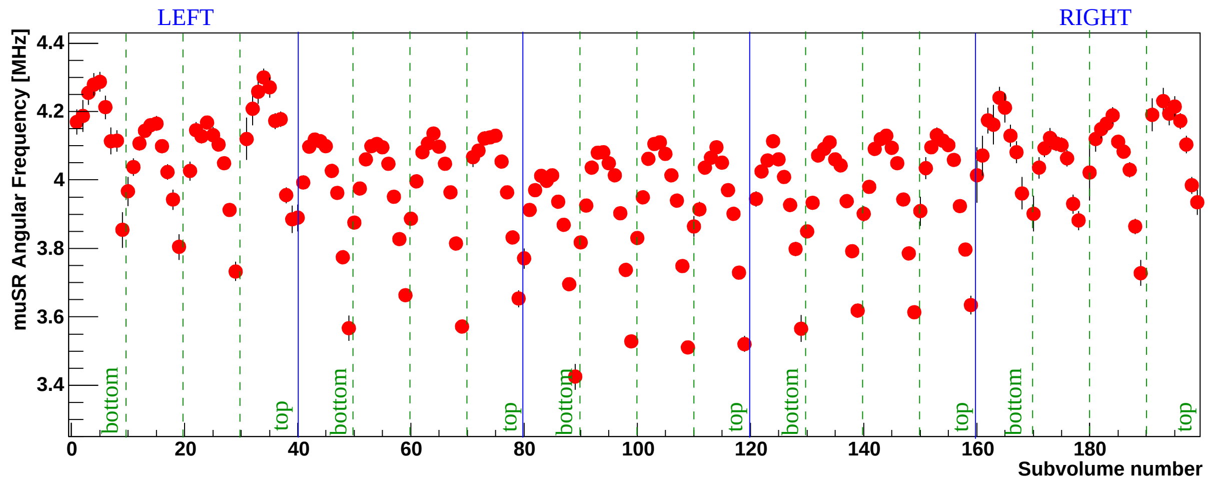

Figure 3: Fitted μSR frequency versus subvolume number: the z coordinate varies fastest, then y, then x.

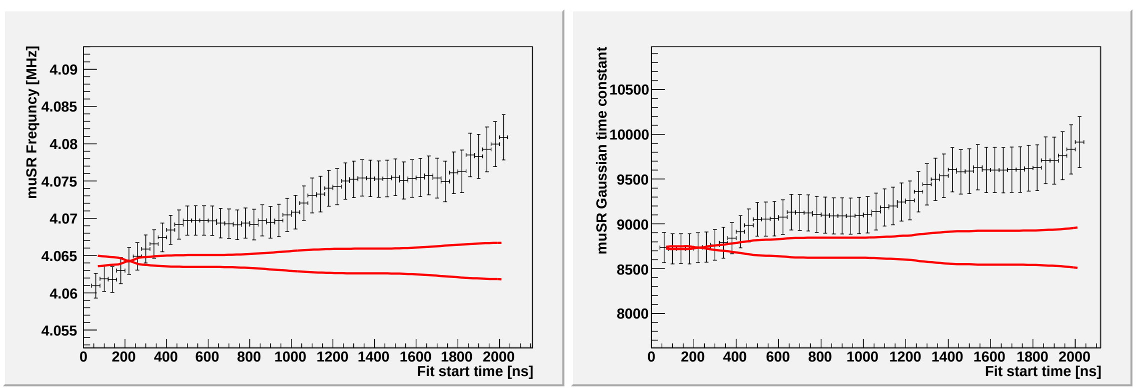

Figure 4: Fitted μSR frequency and Gaussian time constant as a function of fit start time for the Prod50 dataset with only the standard fiducial volume cut, showing that the frequency is not stable in this case. Similar behavior is seen when an exponential μSR envelope $P(t)$ is used.

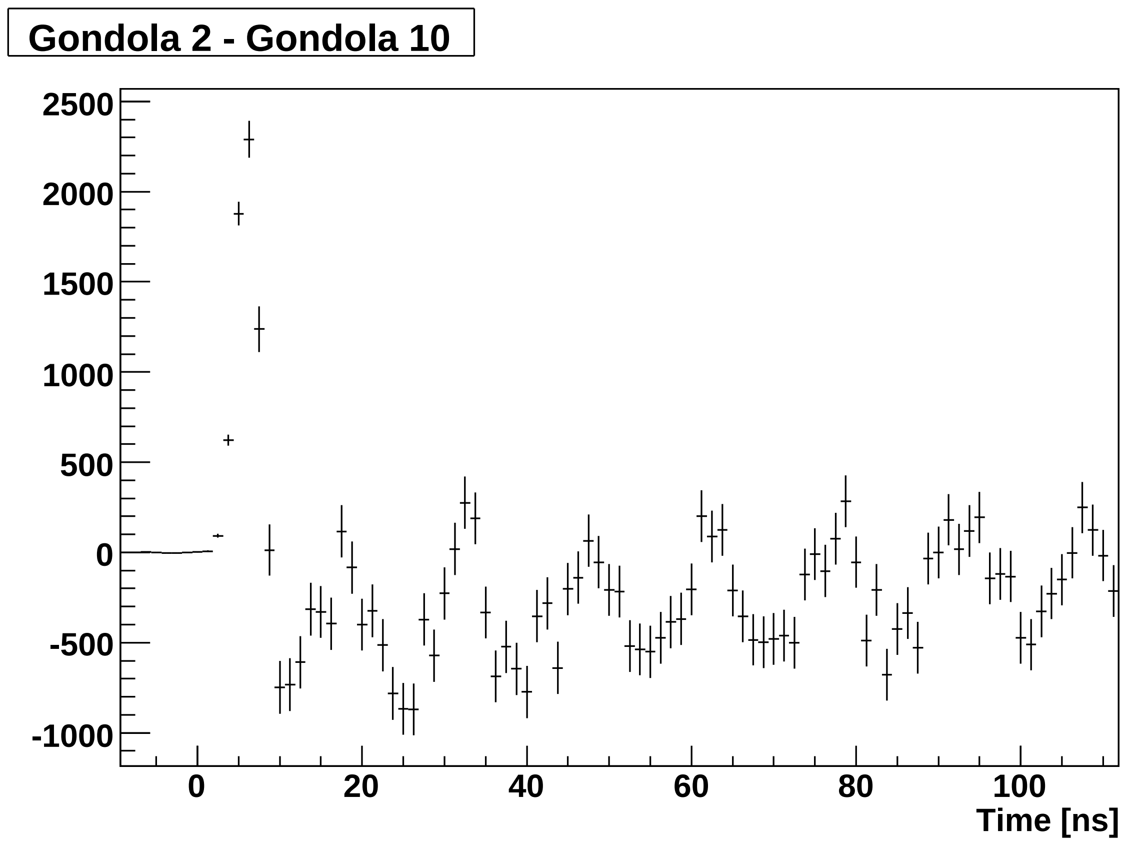

Figure 5: Difference of time spectra from gondola 2 and 10, in fine bins (1.25 ns rather than the typical 40 ns) and at early time. These oscillations correspond to the expected precession frequency of muonium.

Consequently, data sets were constructed with cuts on the muon stopping point in the space (r_μ, z_μ), where $r_\mu^2 = x_\mu^2 + y_\mu^2$; this radial cut tends to exclude the corners of the TPC. A cut of $r_\mu < 60$ mm, 60 mm $> z_\mu >$ 210 mm reduces the field non-uniformity from ∼15% to ∼3%. Lifetime histograms for the following cuts were constructed, in all permutations:

- $r_\mu < 40$ mm, $r_\mu < 50$ mm, $r_\mu < 60$ mm.
- 30 mm $< z_\mu <$ 240 mm, 45 mm $< z_\mu <$ 225 mm, 60 mm $< z_\mu <$ 210 mm.

In addition, a number of variations on the lifetime histograms were built, with different choices on details such as

- ePC cathode inner/outer strips: AND vs. OR
- impact parameter: no cut vs. 120 mm cut
- scatter events: no cut vs. total least squares (TLS) scatter cut vs. multiwire proportional chamber (MWPC) scatter cut vs. OR of TLS and MWPC scatter cuts
- unique electron: no cut vs. requirement of only one electron within 25 μs after the muon.

The default analysis described in this report uses the OR of the ePC cathodes, a 120 mm impact parameter cut, no scatter cut, and no unique electron requirement. These cuts correspond to "study 12" in the context of the Berkeley analysis software. Also, the final result will be based on $r_\mu < 60$ mm and 60 mm $< z_\mu <$ 210 mm.

Figure 6 shows a typical example of the behavior of the μSR parameters as a function of fit start time, using the Gaussian parameterization of the polarization from Equation 4. The earliest fit start time beyond which the fit is stable is typically ∼300 ns. The instability in the fitted μSR frequency at very early fit start times is due at least in part to the fast oscillation of muonium, illustrated in Figure 5. Figure 7 is similar, but it uses an exponential form for $P(t)$ as in Equation 3. The Gaussian time constant is more stable than the exponential lifetime, and the stability of the μSR frequency and the χ^2/dof is similar for the two forms. Consequently, the Gaussian form will be chosen in the end for the final result, although this choice is basically irrelevant: it will be seen that the lifetime values resulting from the two envelope functions are quite consistent.

Similarly, fit stop time scans appear in Figures 8 and 9. They show that there is little additional precision to be gained after the default 15 μs stop time, and that the fits are stable as a function of stop time.

Table 1 summarizes the μSR parameters from fits over the range from 320 ns to 15 μs for both the Prod-50 and All-48 datasets. These values will be used as input to the main fitting procedure described in the next section.

3 Fits to determine lifetime

Lifetime results over a standard fit range from 320 ns to 24.5 μs are summarized in Table 2, using standard cuts. These values arise from fitting each of the 16 gondolas individually and fitting a constant to the resulting 16 lifetimes to determine the appropriately weighted average. In these fits, the parameters $\omega_{\mu SR}$ and $T_{\mu SR}$ are held fixed, and other parameters are allowed to vary. The standard deviation of the reduced χ^2 is much smaller than it would be in the case of a single fit to the sum of the data, and it has been verified that the agreement in the lifetime is at the level of $\sim 10\%$ of the statistical uncertainty. The value of λ is always presented after multiplication by a blinding offset $(1+\delta)$ where $\delta \sim O(10^{-4})$.

The fit start time is constrained by the point where the μSR parameter fits were stable; in fact, the lifetime fits themselves are stable at significantly earlier times, as may be seen in the start time scans in Figures 10 through 13. However, the systematic effects from the muonium relaxation have not been quantified at these times. The potential gain in statistical precision by moving the fit start time from 320 ns to 40 ns would be a change from an uncertainty of 33.6 Hz to 31.4 Hz for the Prod-50 data and from 37.2 Hz to 34.8 Hz for the All-48 data.

Fit stop time scans appear in Figures 14 through 17. The lifetime and χ^2/dof appear to be stable as a function of fit stop time, but the background parameter B does not. A systematic uncertainty will be assigned to account for this apparent time dependence of the background.

Prod-50 data:

r cut (mm)	z cut (mm)	$\omega_{\mu SR}$ (MHz) (exponential)	$\tau_{\mu SR}$ (μs)	$\omega_{\mu SR}$ (MHz) (Gaussian)	$T_{\mu SR}$ (μs)
40	30-240	4.0564 ± 0.0020	34.0 ± 2.3	4.0558 ± 0.0021	11.9 ± 0.4
50	30-240	4.0606 ± 0.0018	35.4 ± 2.2	4.0601 ± 0.0018	12.2 ± 0.4
60	30-240	4.0648 ± 0.0017	36.4 ± 2.2	4.0643 ± 0.0017	12.3 ± 0.4
40	45-225	4.0613 ± 0.0020	49.3 ± 5.0	4.0611 ± 0.0020	14.5 ± 0.8
50	45-225	4.0660 ± 0.0018	52.7 ± 5.1	4.0658 ± 0.0018	15.1 ± 0.7
60	45-225	4.0703 ± 0.0017	54.9 ± 5.1	4.0701 ± 0.0017	15.3 ± 0.7
40	60-210	4.0737 ± 0.0021	60.9 ± 8.4	4.0736 ± 0.0021	16.7 ± 1.2
50	60-210	4.0780 ± 0.0019	68.7 ± 9.6	4.0779 ± 0.0019	17.9 ± 1.3
60	60-210	4.0823 ± 0.0018	70.0 ± 9.6	4.0821 ± 0.0018	18.0 ± 1.3

All-48 data:

r cut (mm)	z cut (mm)	$\omega_{\mu SR}$ (MHz) (exponential)	$\tau_{\mu SR}$ (μs)	$\omega_{\mu SR}$ (MHz) (Gaussian)	$T_{\mu SR}$ (μs)
40	30-240	4.0589 ± 0.0022	44.2 ± 4.2	4.0591 ± 0.0022	13.7 ± 0.7
50	30-240	4.0629 ± 0.0019	46.9 ± 4.3	4.0629 ± 0.0020	14.2 ± 0.7
60	30-240	4.0662 ± 0.0019	47.7 ± 4.2	4.0661 ± 0.0019	14.3 ± 0.7
40	45-225	4.0634 ± 0.0021	61.5 ± 8.7	4.0636 ± 0.0021	15.9 ± 1.1
50	45-225	4.0672 ± 0.0019	67.5 ± 9.4	4.0674 ± 0.0019	17.0 ± 1.2
60	45-225	4.0708 ± 0.0018	69.1 ± 9.1	4.0709 ± 0.0019	17.2 ± 1.2
40	60-210	4.0744 ± 0.0022	68.2 ± 14.2	4.0745 ± 0.0022	16.6 ± 1.7
50	60-210	4.0779 ± 0.0020	90.2 ± 17.6	4.0781 ± 0.0020	18.4 ± 1.9
60	60-210	4.0812 ± 0.0019	96.5 ± 18.6	4.0813 ± 0.0019	19.5 ± 2.0

Table 1: μSR parameters that will be used in the primary fits to determine the muon lifetime. They were determined over a fitting range of 320 ns to 15 μs using the default treatment: ePC cathode OR, 120 mm impact parameter cut, no scatter cut, and no unique electron requirement, $r_\mu < 60$ mm, and 60 mm $< z_\mu <$ 210 mm.

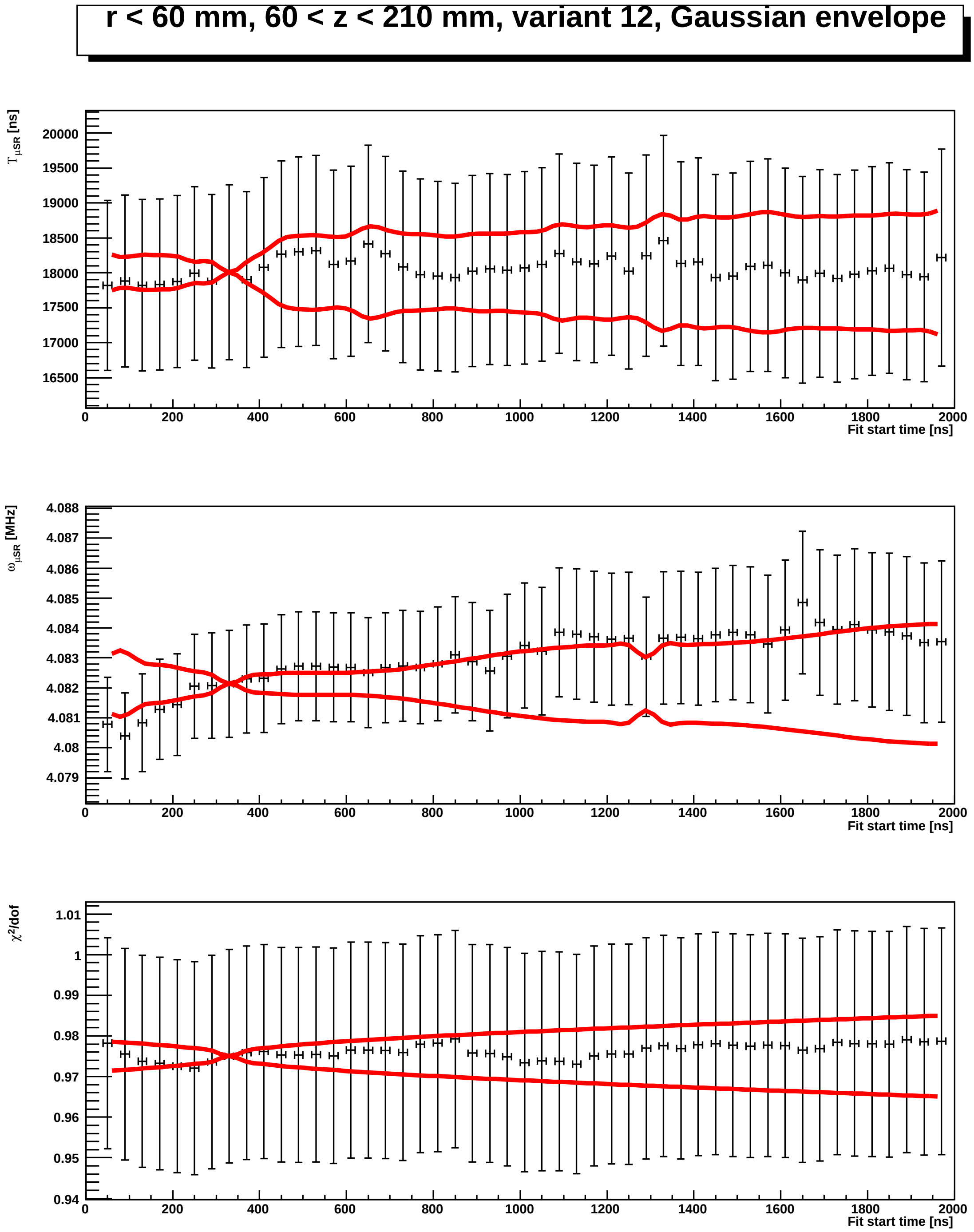

Figure 6: Start time scan for μSR parameters for the Prod-50 data and a Gaussian envelope function. The fit stop time is 15 μs.

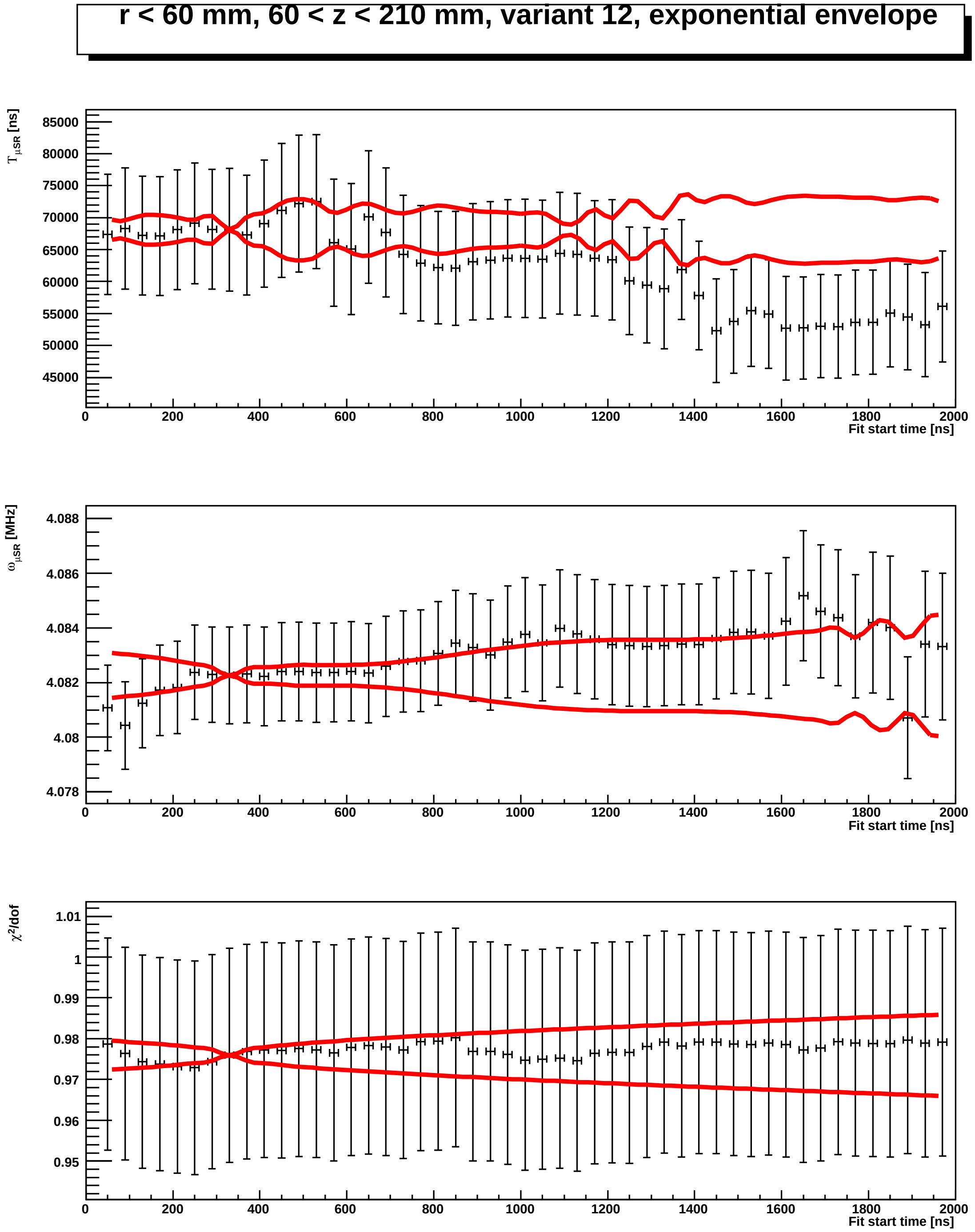

Figure 7: Start time scan for μSR parameters for the Prod-50 data and an exponential envelope function. The fit stop time is 15 μs.

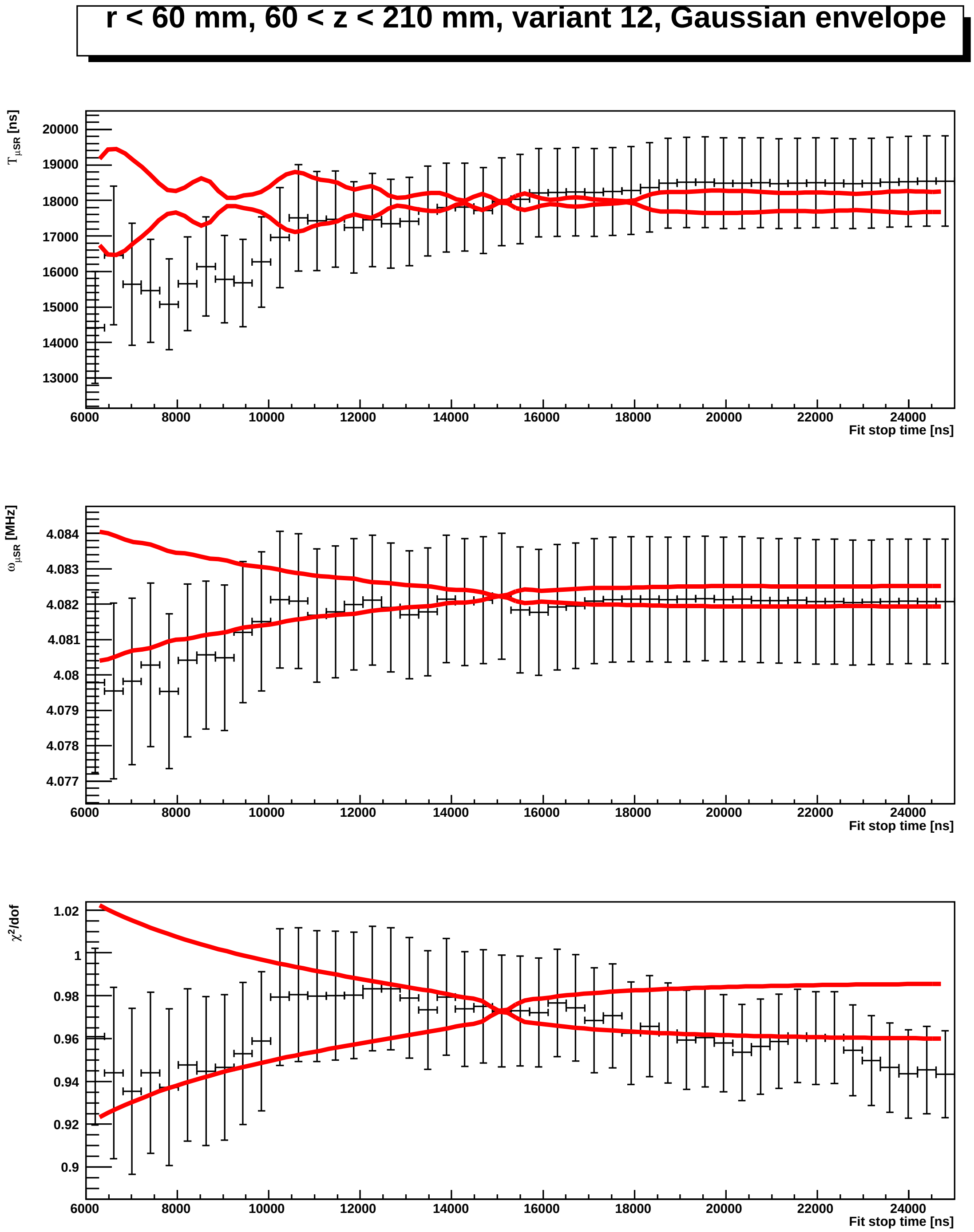

Figure 8: Stop time scan for μSR parameters for the Prod-50 data and a Gaussian envelope function. The fit start time is 320 ns.

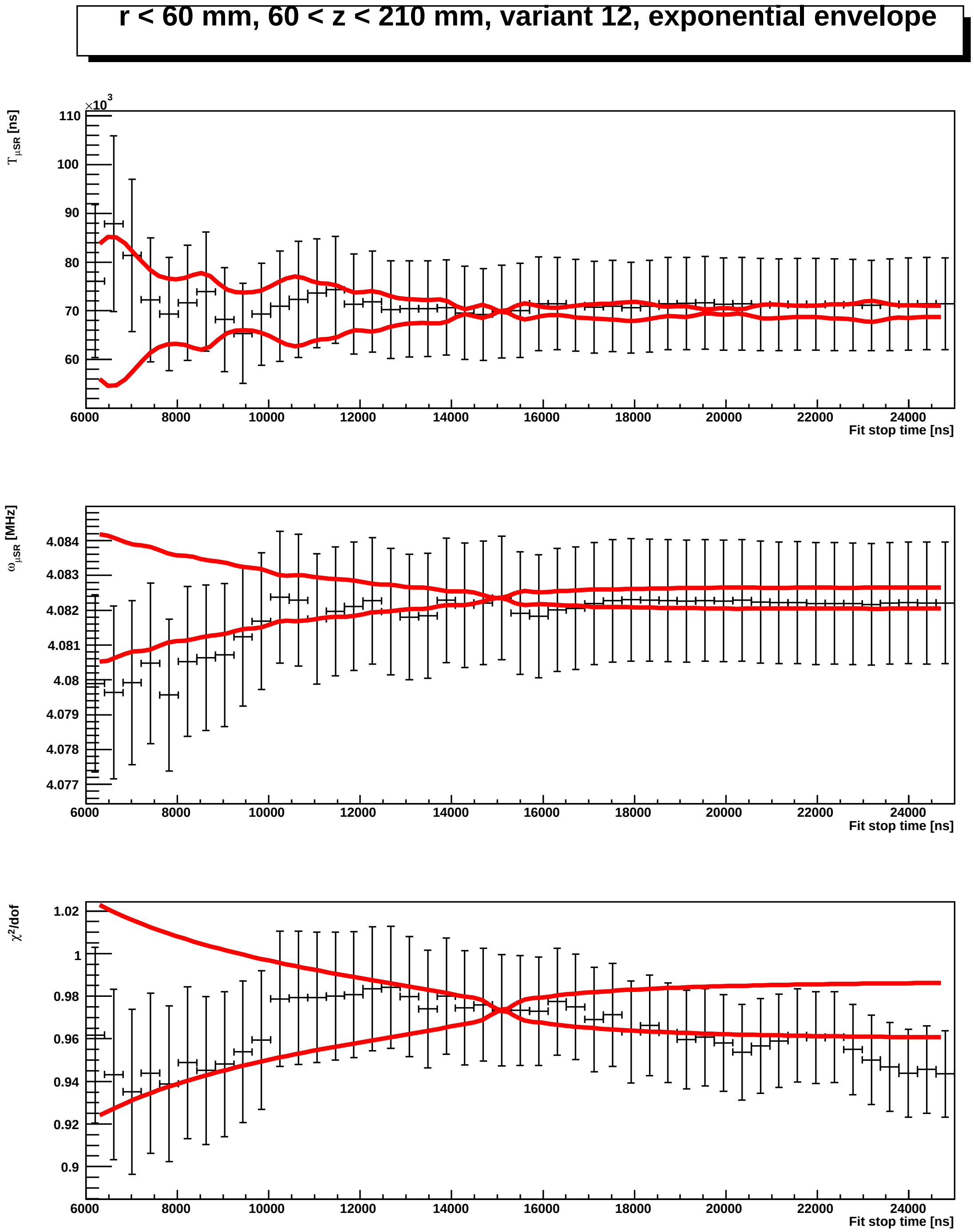

Figure 9: Stop time scan for μSR parameters for the Prod-50 data and an exponential envelope function. The fit start time is 320 ns.

Prod-50 data:

r cut (mm)	z cut (mm)	λ (kHz) (exponential)	χ^2/dof	λ (kHz) (Gaussian)	χ^2/dof
40	30-240	454.7974 ± 0.0352	1.007 ± 0.014	454.7958 ± 0.0352	1.007 ± 0.014
50	30-240	454.7995 ± 0.0316	1.002 ± 0.014	454.7980 ± 0.0315	1.001 ± 0.014
60	30-240	454.7952 ± 0.0303	1.002 ± 0.014	454.7938 ± 0.0303	1.001 ± 0.014
40	45-225	454.7888 ± 0.0364	1.011 ± 0.014	454.7878 ± 0.0364	1.011 ± 0.014
50	45-225	454.7916 ± 0.0326	1.004 ± 0.014	454.7907 ± 0.0326	1.003 ± 0.014
60	45-225	454.7886 ± 0.0314	1.003 ± 0.014	454.7877 ± 0.0313	1.003 ± 0.014
40	60-210	454.7704 ± 0.0390	1.008 ± 0.014	454.7698 ± 0.0390	1.008 ± 0.014
50	60-210	454.7823 ± 0.0349	0.993 ± 0.014	454.7817 ± 0.0349	0.993 ± 0.014
60	60-210	454.7815 ± 0.0336	0.996 ± 0.014	454.7810 ± 0.0336	0.995 ± 0.014

All-48 data:

r cut (mm)	z cut (mm)	λ (kHz) (exponential)	χ^2/dof	λ (kHz) (Gaussian)	χ^2/dof
40	30-240	454.7109 ± 0.0389	1.023 ± 0.014	454.7101 ± 0.0388	1.024 ± 0.014
50	30-240	454.7276 ± 0.0350	1.031 ± 0.014	454.7268 ± 0.0350	1.031 ± 0.014
60	30-240	454.7151 ± 0.0337	1.025 ± 0.014	454.7142 ± 0.0337	1.025 ± 0.014
40	45-225	454.7091 ± 0.0400	1.016 ± 0.014	454.7086 ± 0.0400	1.017 ± 0.014
50	45-225	454.7251 ± 0.0361	1.024 ± 0.014	454.7245 ± 0.0361	1.024 ± 0.014
60	45-225	454.7148 ± 0.0348	1.020 ± 0.014	454.7143 ± 0.0348	1.020 ± 0.014
40	60-210	454.7164 ± 0.0428	1.019 ± 0.014	454.7162 ± 0.0428	1.019 ± 0.014
50	60-210	454.7331 ± 0.0386	1.019 ± 0.014	454.7328 ± 0.0386	1.019 ± 0.014
60	60-210	454.7234 ± 0.0372	1.016 ± 0.014	454.7231 ± 0.0371	1.016 ± 0.014

Table 2: Results of fits to determine the lifetime as a function of spatial cut on the muon stopping point. All values are displayed with a multiplicative offset.

For the selected spatial cuts of $r < 60$ mm, 60 mm $< z <$ 210 mm, the lifetime values are (with statistical errors only)

$$\lambda_{Prod-50} = 454.7815 \pm 0.0336\,\text{kHz}$$

and

$$\lambda_{All-48} = 454.7234 \pm 0.0372\,\text{kHz}.$$

The difference between these values is 0.0581 ± 0.0501 Hz, so they are consistent. The combined result is then

$$\lambda = 454.755 \pm 0.0249\,\text{kHz (stat.)}.$$

4 Systematic uncertainties

4.1 Muon spin rotation

The uncertainty in the μSR frequency and lifetime needs to be propagated into the final result. Figure 20 shows the dependence of the lifetime and χ^2/dof on these parameters. The systematic uncertainty is determined by subtracting the point where the fixed parameter is set to -2 standard deviations from the point at the central value of the fixed parameter.

Dataset	$\delta\lambda_o$ from $T_{\mu SR}$ [Hz]	$\delta\lambda_o$ from $\omega_{\mu SR}$ [Hz]	$\delta\lambda_o$ (combined) [Hz]
Prod-50	0.28	0.20	0.34
All-48	0.35	0.15	0.38

The conclusion is that the 2σ systematic uncertainty for the combined dataset is $\pm$ 0.36 Hz.

4.2 Electron detector treatment

Figures 21 and 22 show the dependence of the result on variations in the data processing algorithm. The difference between the ePC cathode AND and ePC cathode OR results (with 120 mm impact cut and no scatter cut) is 13.4±9.7 Hz for the Prod-50 dataset and 10.4±10.7 Hz for the All-48 dataset. The indicated uncertainty is the correlated error given by the Kawall formula. Consequently, there is no evidence of any dependence on the electron detector treatment.

4.3 Time-dependent background

The behavior of the background parameter in the fit stop time scans suggests that there may be a time-dependent component of the background. Also, the variations on the dataset preparation that lead to higher background levels seem to give higher values for the decay rate as well. For example, for the Prod-50 data, imposing the 120 mm impact parameter cut reduces the background by a factor of 2.9 and the decay rate by 8.5 $\pm$ 4.2 Hz. For the All-48 data, the background is again reduced by a factor of 2.9 and the decay rate by 15.6 $\pm$ 4.8 Hz, which seems to be significant.

The origin of this discrepancy is not at all clear. For the moment, it will be covered by asssigning a systematic uncertainty of 12.1 Hz (the average of the 8.5 Hz and 15.6 Hz) to the time-dependent background.

4.4 Others

Several other systematic uncertainties estimates will be “inheirited” from the μ^- analysis:

- Muon stop definition
- Muon detector inefficiencies
- Electron detector inefficiencies
- Electronics and beam structure (a new report on this topic will appear soon)

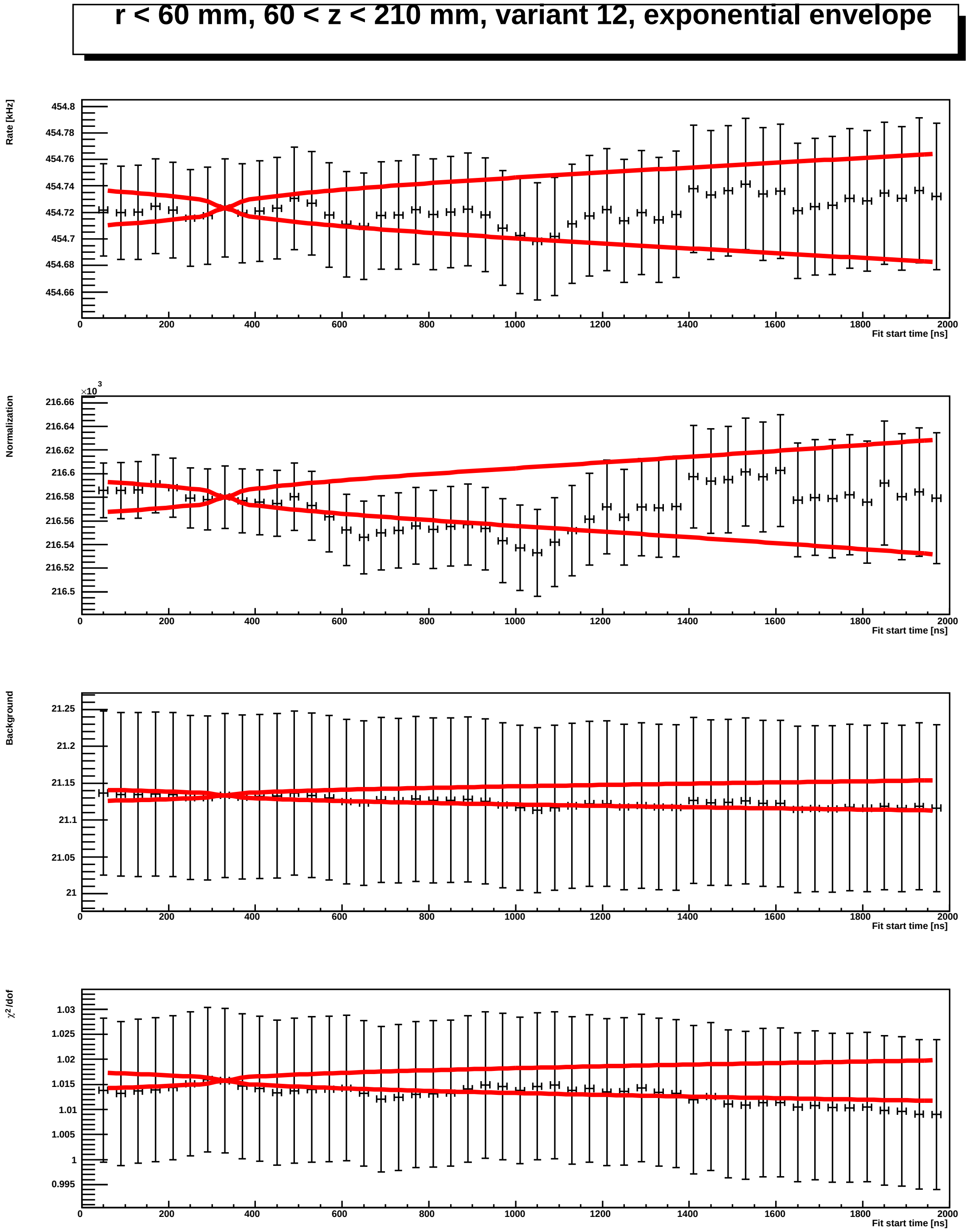

Figure 10: Start time scan for lifetime parameters: 24.5 μs stop time, $r < 60$mm, $60 < z < 210$ mm, All-48 data, ePC cathode OR, 120 mm impact cut, exponential envelope.

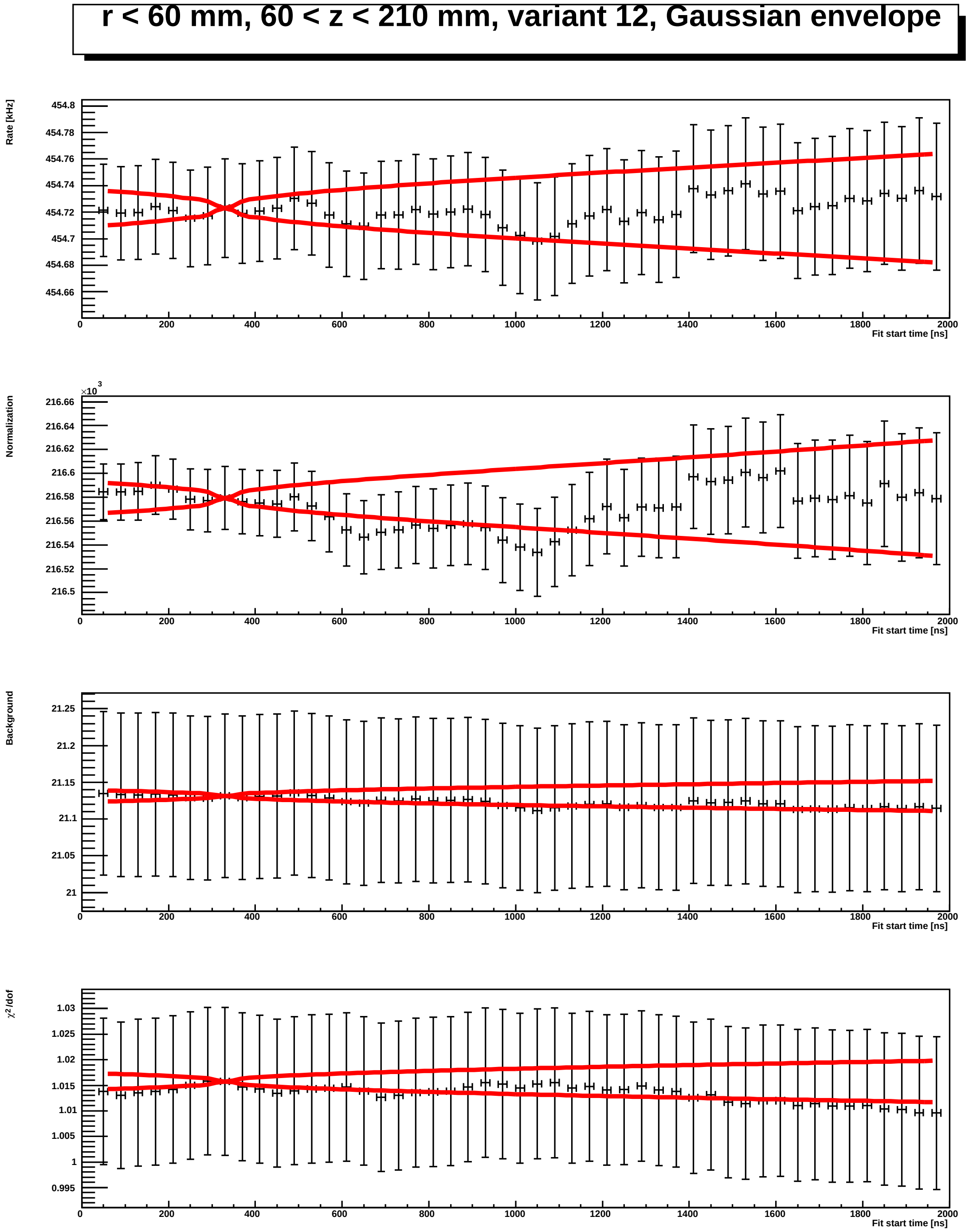

Figure 11: Start time scan for lifetime parameters: 24.5 μs stop time, $r < 60$mm, $60 < z < 210$ mm, All-48 data, ePC cathode OR, 120 mm impact cut, Gaussian envelope.

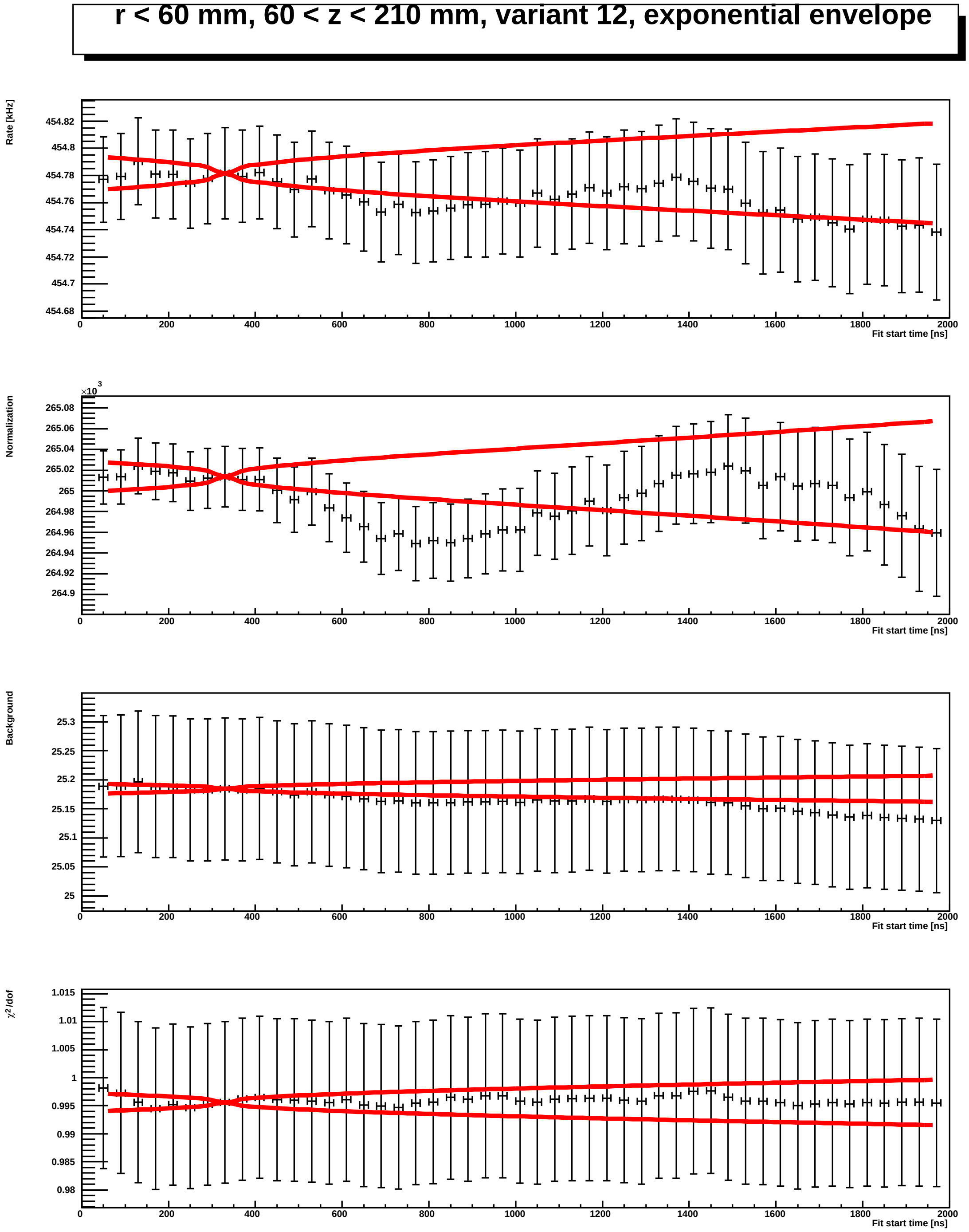

Figure 12: Start time scan for lifetime parameters: 24.5 μs stop time, $r < 60$mm, $60 < z < 210$ mm, Prod-50 data, ePC cathode OR, 120 mm impact cut, exponential envelope.

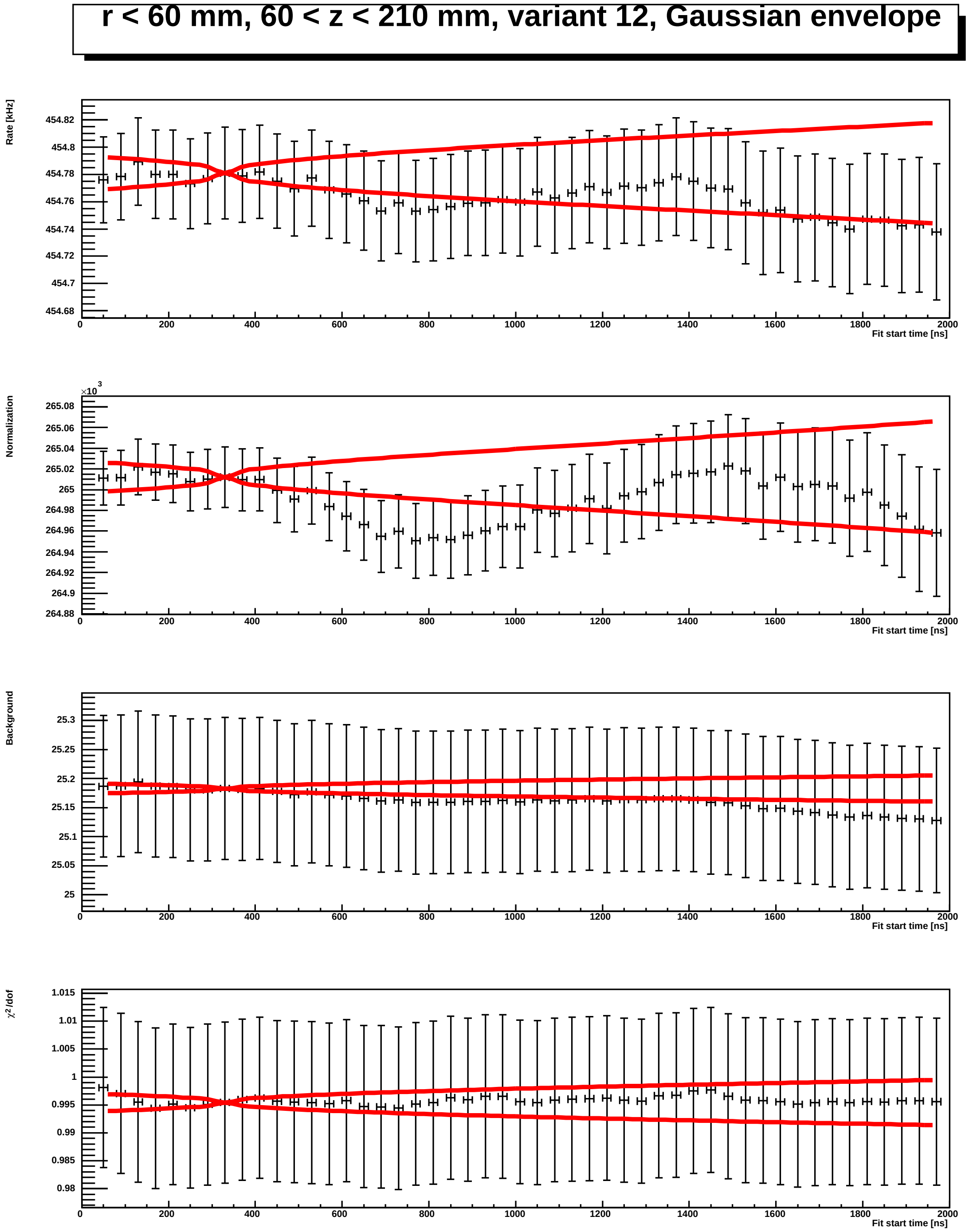

Figure 13: Start time scan for lifetime parameters: 320 ns start time, $r < 60$mm, $60 < z < 210$ mm, Prod-50 data, ePC cathode OR, 120 mm impact cut, Gaussian envelope.

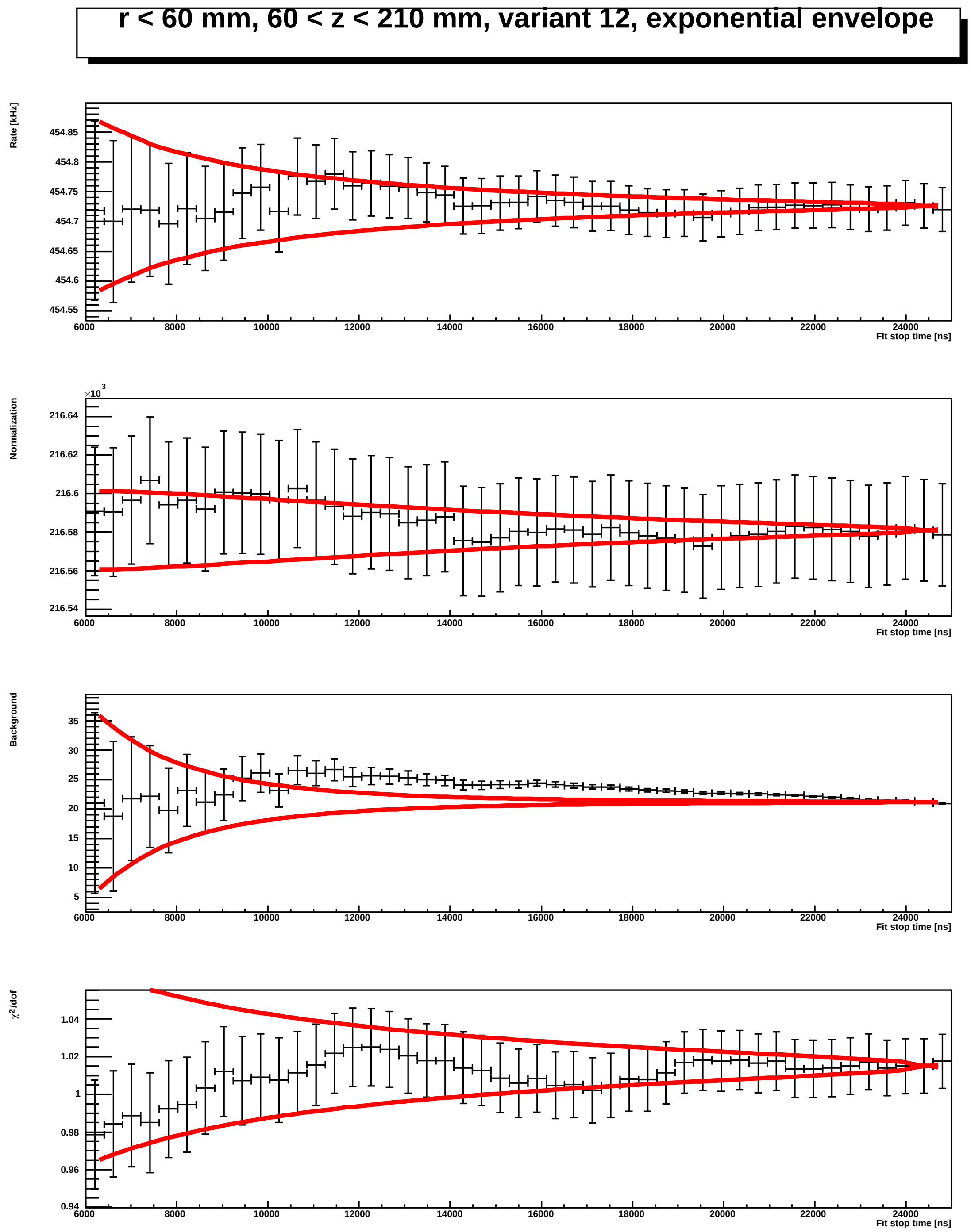

Figure 14: Stop time scan for lifetime parameters: 320 ns start time, $r < 60$mm, $60 < z < 210$ mm, All-48 data, ePC cathode OR, 120 mm impact cut, exponential envelope.

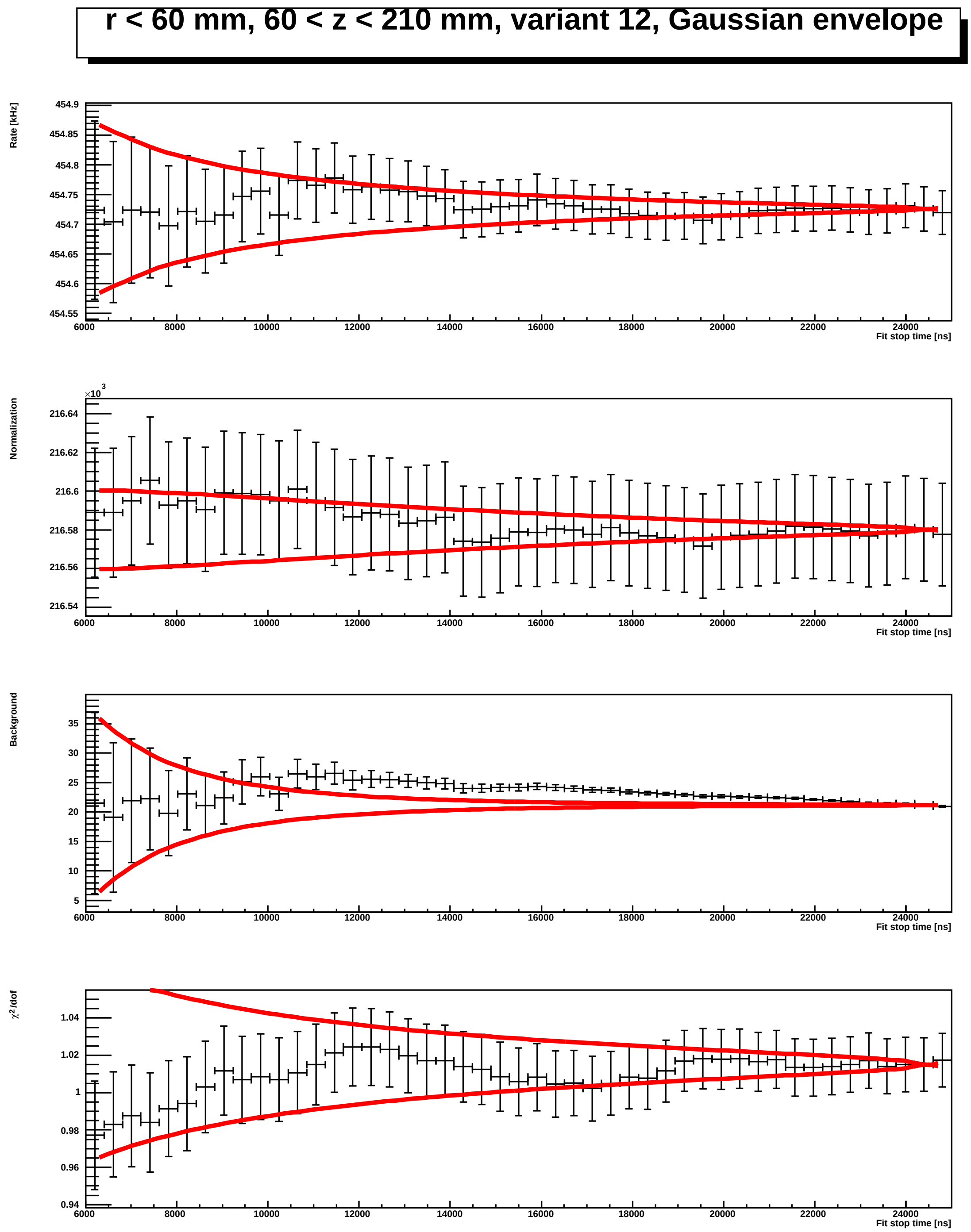

Figure 15: Stop time scan for lifetime parameters: 320 ns start time, $r < 60$mm, $60 < z < 210$ mm, All-48 data, ePC cathode OR, 120 mm impact cut, Gaussian envelope.

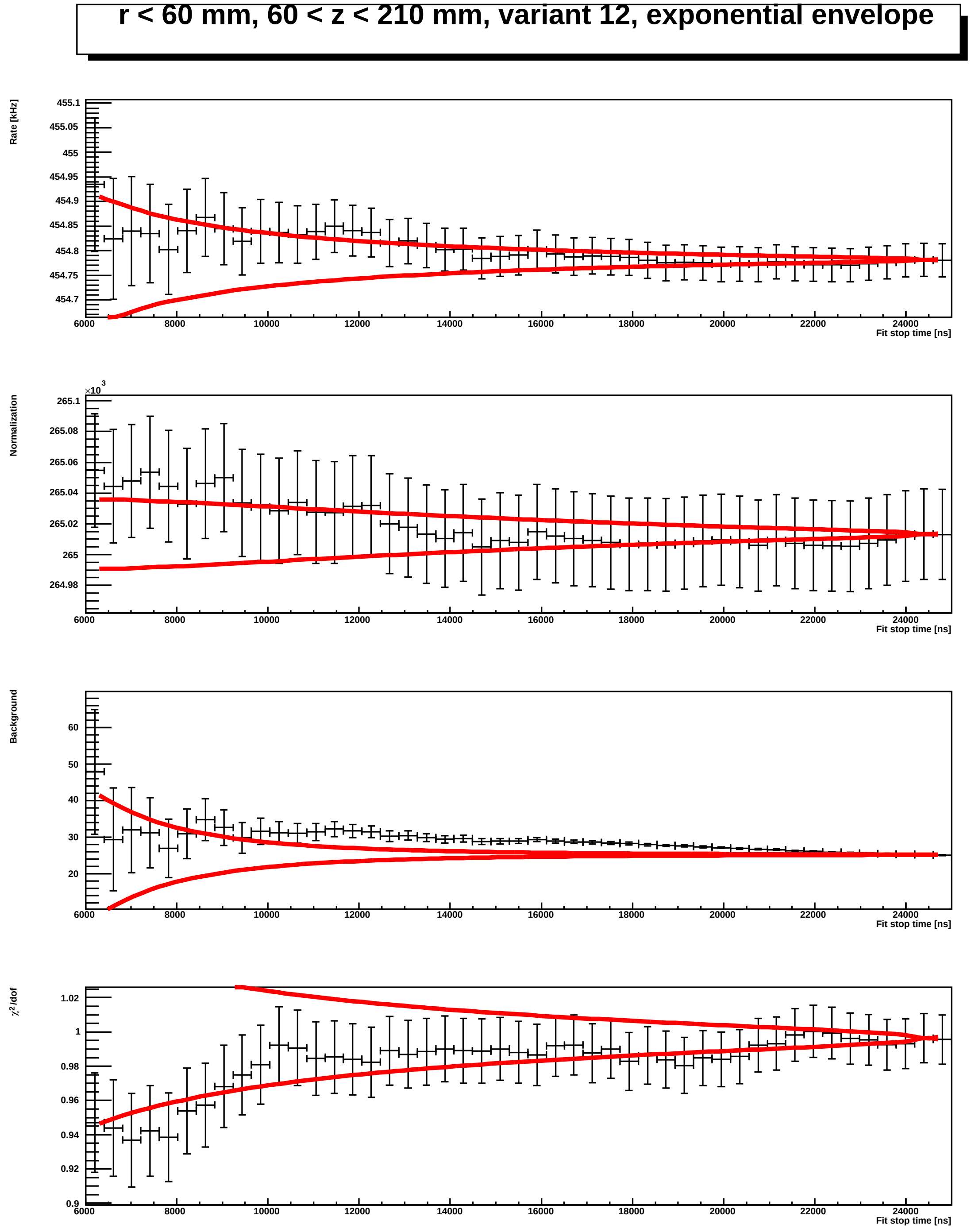

Figure 16: Stop time scan for lifetime parameters: 320 ns start time, $r < 60$mm, $60 < z < 210$ mm, Prod-50 data, ePC cathode OR, 120 mm impact cut, exponential envelope.

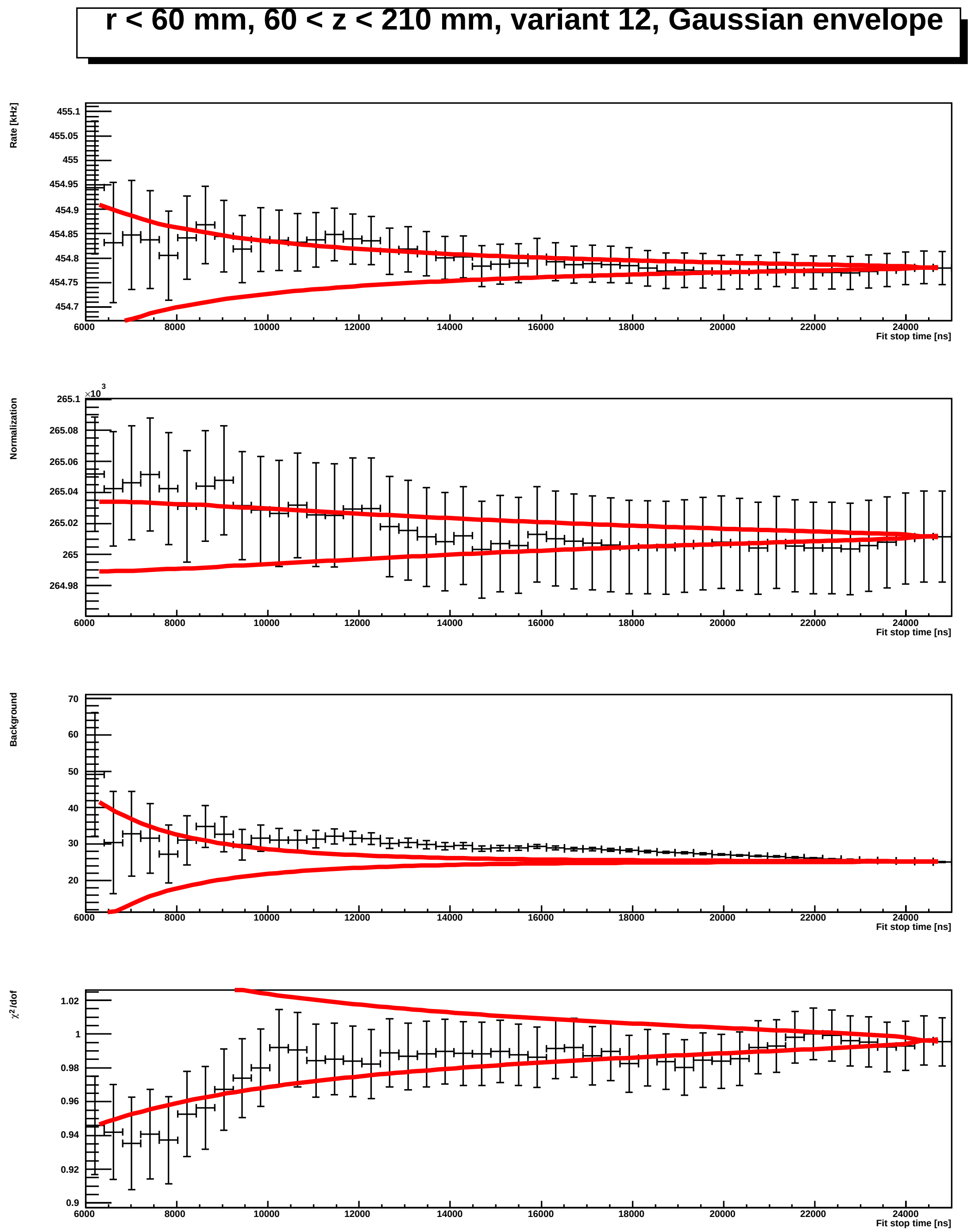

Figure 17: Stop time scan for lifetime parameters: 320 ns start time, $r < 60$mm, $60 < z < 210$ mm, Prod-50 data, ePC cathode OR, 120 mm impact cut, Gaussian envelope.

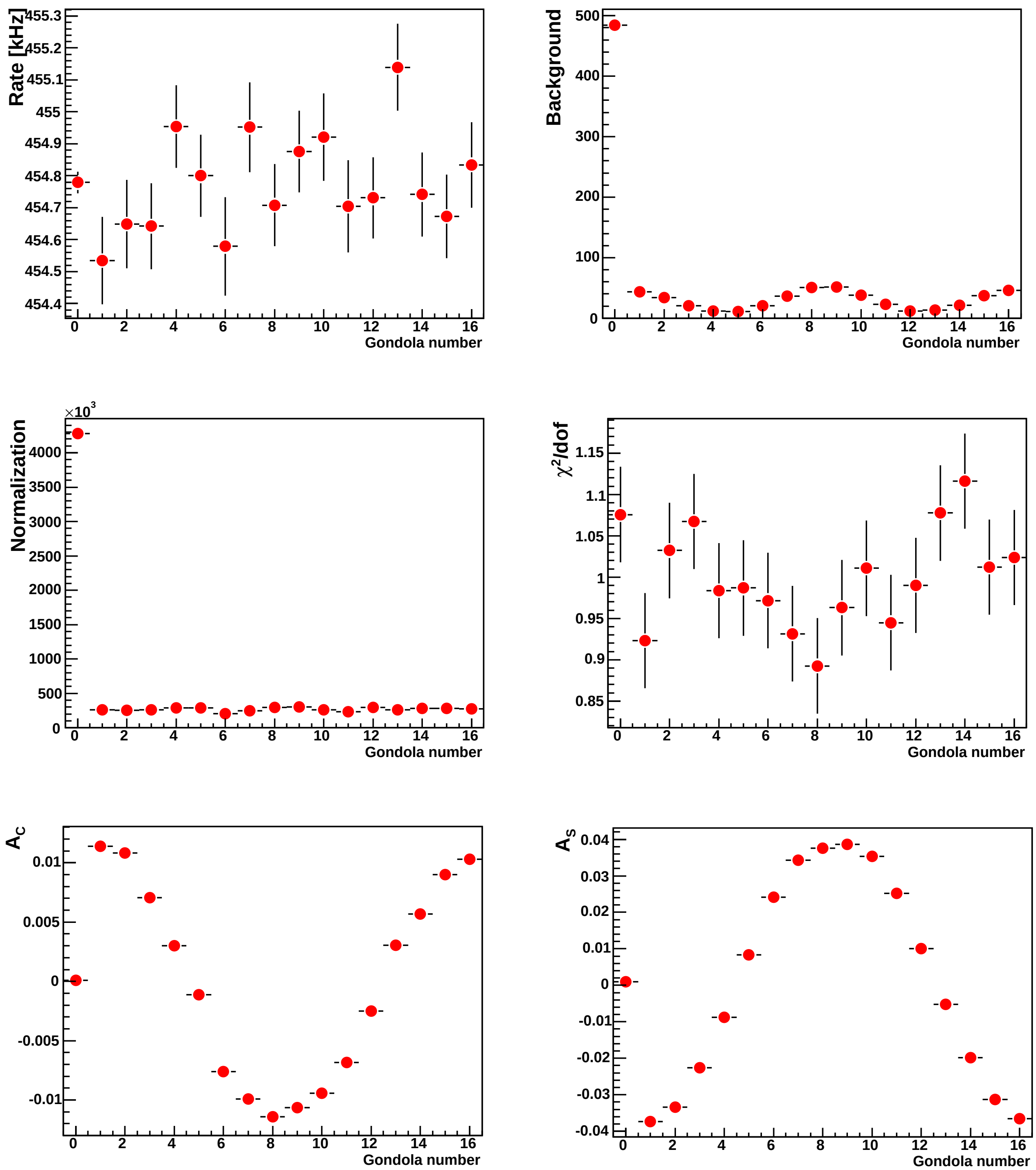

Figure 18: Typical distribution of fit parameters by gondola. (Prod-50 data, $r < 60$ mm, 60 mm $< z <$ 210 mm, 320 ns $< t <$ 24.5 μs, Gaussian form).

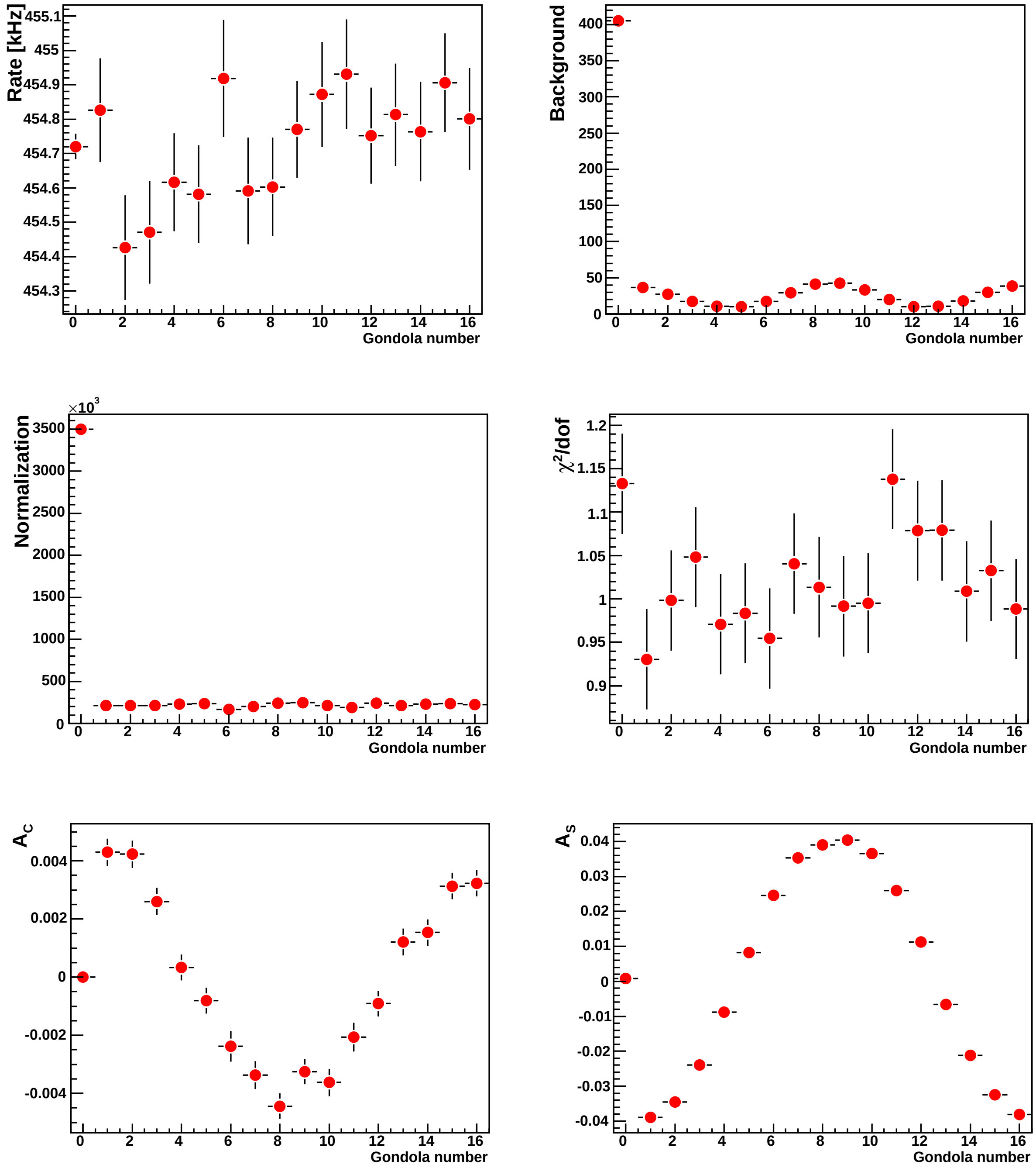

Figure 19: Typical distribution of fit parameters by gondola. (All-48 data, $r < 60$ mm, 60 mm $< z <$ 210 mm, 320 ns $< t <$ 24.5 μs, Gaussian form).

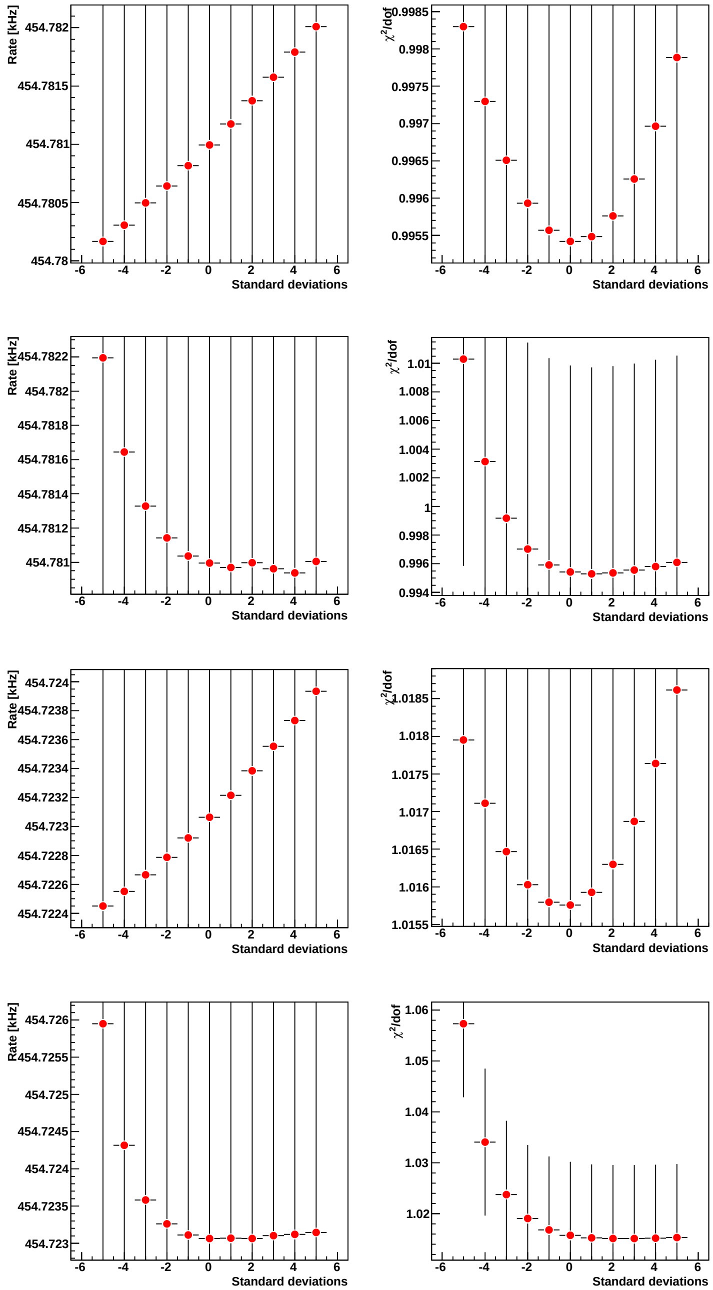

Figure 20: Fitted λ and χ^2/dof for varying $\omega_{\mu SR}$ or $T_{\mu SR}$. From top to bottom: (a) Prod-50 $\omega_{\mu SR}$; (b) Prod-50 $T_{\mu SR}$; (c) All-48 $\omega_{\mu SR}$; (d) All-48 $T_{\mu SR}$. The units of the horizontal axis represent the 1σ uncertainty of the fixed parameter and are taken relative to the fixed parameter's central value.

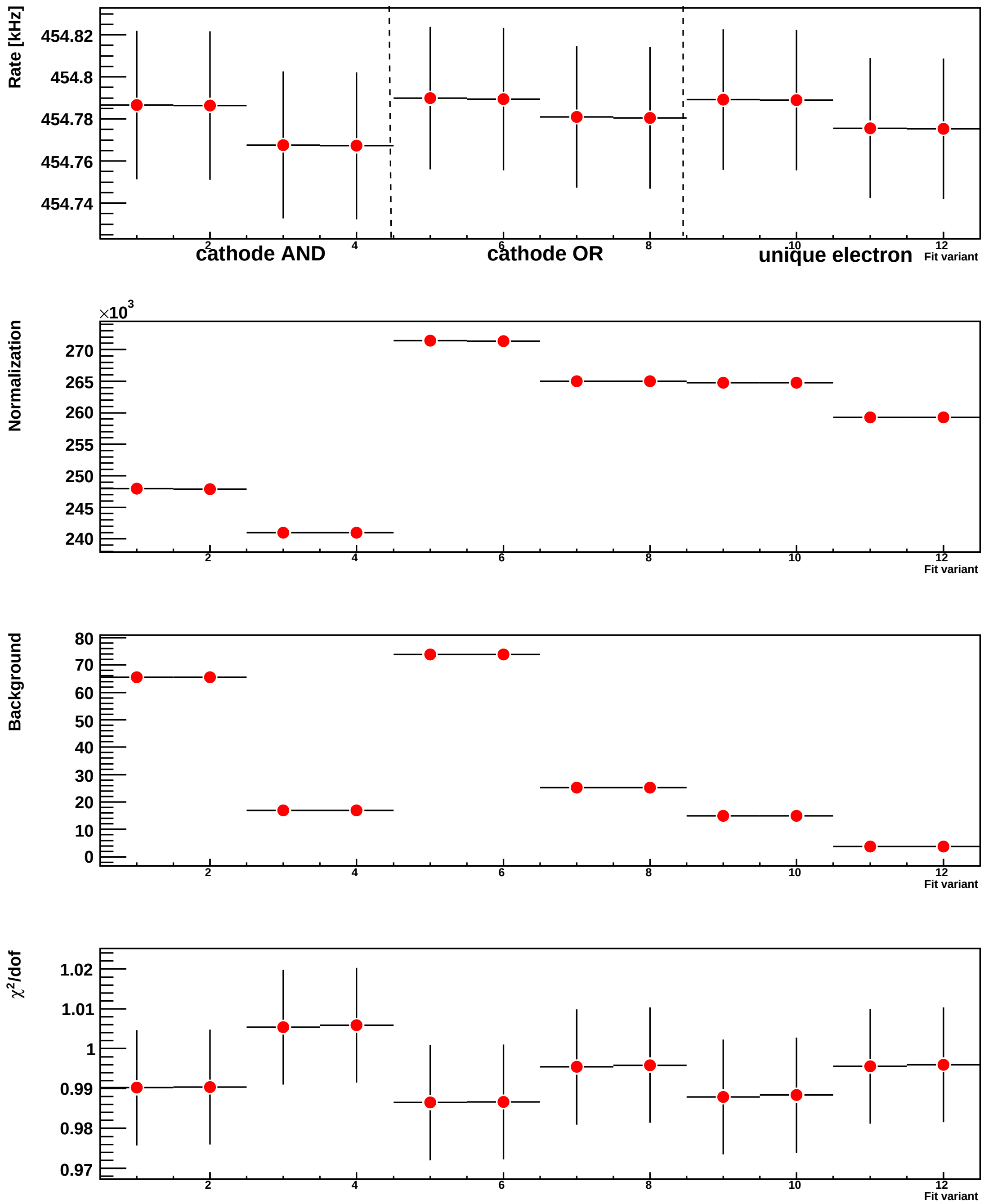

Figure 21: Fits to the Prod-50 dataset with variations in the dataset preparation. There are three groups of four points. The groups correspond to ePC cathode AND, ePC cathode OR, and ePC cathode OR with a unique electron requirement. Within each group, the first two points have no impact parameter cut, while the second two have a 120 mm impact parameter cut. The first point of each pair has no scatter cut, while the second one does (TLS OR MWPC).

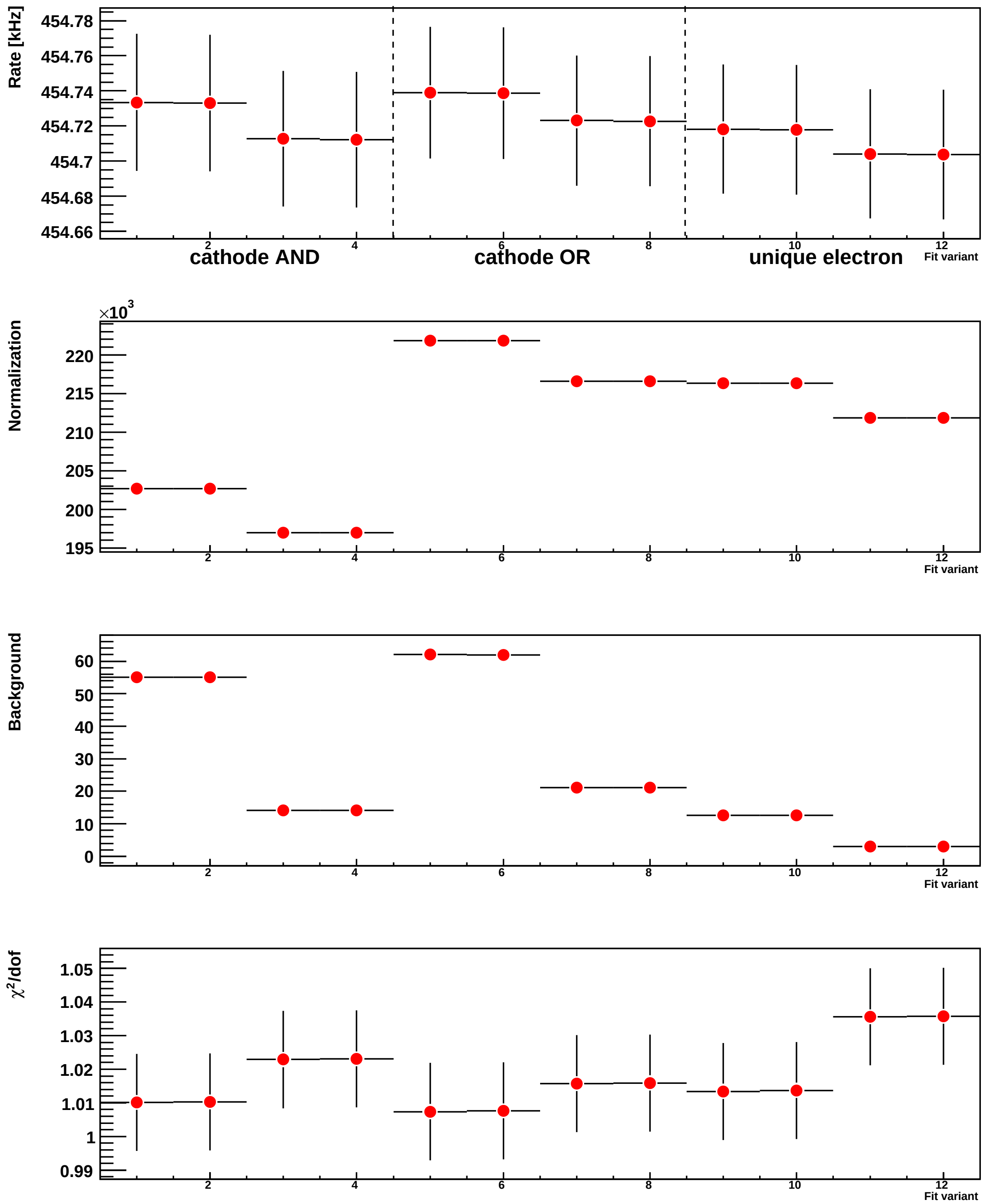

Figure 22: Fits to the All-48 dataset with variations in the dataset preparation. There are three groups of four points. The groups correspond to ePC cathode AND, ePC cathode OR, and ePC cathode OR with a unique electron requirement. Within each group, the first two points have no impact parameter cut, while the second two have a 120 mm impact parameter cut. The first point of each pair has no scatter cut, while the second one does (TLS OR MWPC).

5 Summary

In summary, this report recommends a value for the μ^+ decay rate of

$$\lambda_o = 454.755 \pm 0.0249\,(\text{stat.}) \pm 0.0131(\text{syst.})\ \text{kHz}$$

This value is displayed with a small multiplicative offset known to the author. It arises from the combination of data from Prod-50, Prod-48, and CalibD2-48 data subsets. The systematic uncertainty is dominated by a lack of understanding of some time-dependent structure in the background that may couple to the decay rate. Other contributions to the systematic uncertainty are given in Table 3.

Time dependent background	12.1 Hz
Electronics and beam structure	$\sim$5 Hz
μSR parameters	0.4 Hz
Muon stop definition	?
Muon detector inefficiencies	?
Electron detector inefficiencies	?
Total	13.1 Hz

Table 3: Summary of systematic uncertainties considered in this analysis.